UDC 532.8

A. B. Lysenko*, O. L. Kosynska, D. G. Skipochka

Dniprodzerzhinsk State Technical University, Kamenskoe, Ukraine
**e-mail: ablysenko@ukr.net*

THERMAL REGIMES AND CRYSTALLIZATION KINETICS OF $Mg_{65}Cu_{25}Y_{10}$ ALLOY AT CASTING IN A METAL MOLD

The computational analysis results of the crystallization kinetics of bulk-amorphizing $Mg_{65}Cu_{25}Y_{10}$ alloy in casting conditions in a copper mold with 15 mm thickness of heat-removing walls are presented. It is shown that the solidification process is carried out under the influence of different thermal conditions depending on the cast thickness. Such conditions cause the formation of three microstructure types: conditional amorphous, amorphous-nanocrystalline, and microcrystalline. The dependences of the crystallized volume fraction, volume density of the crystals and their averaged sizes on the half-thickness of castings in the range from 0.8 to 8.0 mm are obtained. The accordance of the calculated estimates of thickness and cooling rate of castings, solidifying with forming the negligible volume fraction ($\sim 10^{-6}$) of the crystalline phase, with known experimental data is achieved.

Keywords: Mg65Cu25Y10 alloy castings, mathematical modeling, thermal regimes, crystallization kinetics, types of microstructure.

Наведено результати розрахункового аналізу кінетики кристалізації сплаву $Mg_{65}Cu_{25}Y_{10}$, що об'ємно аморфізується, в умовах лиття в мідну виливницю з товщиною тепловідвідних стінок 15 мм. Показано, що в залежності від товщини відливків процес твердіння здійснюється під дією різних термічних режимів, які обумовлюють формування трьох різновидів мікроструктури: умовно аморфної, аморфно-нанокристалічної та мікрокристалічної. Отримані залежності частини закристалізованого об'єму, об'ємної густини кристалів та їх усереднених розмірів від напівтовщини відливків в інтервалі від 0,8 до 8,0 мм. Досягнуто відповідність розрахункових оцінок товщини та швидкості охолодження відливків, що тверднуть з утворенням нехтовно малої ($\sim 10^{-6}$) об'ємної частки кристалічної фази, відомим експериментальним даним.

Ключові слова: відливки сплаву $Mg_{65}Cu_{25}Y_{10}$, математичне моделювання, термічні режими, кінетика кристалізації, типи мікроструктури.

Представлены результаты расчетного анализа кинетики кристаллизации объемно-аморфизирующегося сплава $Mg_{65}Cu_{25}Y_{10}$ в условиях литья в медную изложницу с толщиной теплоотводящих стенок 15 мм. Показано, что в зависимости от толщины отливок процесс затвердевания осуществляется под действием различных термических режимов, которые обусловливают формирование трех разновидностей микроструктуры: условно аморфной, аморфно-нанокристаллической и микрокристаллической. Получены зависимости доли закристаллизовавшегося объема, объемной плотности кристаллов и их усредненных размеров от полутолщины отливок в интервале от 0,8 до 8,0 мм. Достигнуто согласие расчетных оценок толщины и скорости охлаждения отливок, затвердевающих с образованием ничтожно малой ($\sim 10^{-6}$) объемной доли кристаллической фазы, с известными экспериментальными данными.

Ключевые слова: отливки сплава $Mg_{65}Cu_{25}Y_{10}$, математическое моделирование, термические режимы, кинетика кристаллизации, типы микроструктуры.

1. Introduction

The creation of metallic materials with metastable structures and unique set of properties by methods of quenching from the liquid state (QLS) refers to the priority areas of metal physics and modern metallurgical technologies. One of the latest QLS advances is the development of a new class of amorphous materials - bulk metallic glasses (BMG) [1-3]. In contrast to amorphous thin films obtained by melt spinning methods at cooling rates of $\upsilon_m \approx (10^5 – 5 \cdot 10^6)$ K/s, these materials solidify without crystallization in conditions of casting fabrication with section of several tens of millimeters that, according to [4], corresponds to the value of $\upsilon_m \approx (10^{-1} – 5 \cdot 10^3)$ K/s.

The possibility of amorphous state fixing at relatively low cooling rates of melt suggests that bulk-amorphizing composites are characterized by much lower values of the nucleation and crystal growth in comparison with the pure metals and alloys with an average level of glass-forming ability. The latter allows using the materials of this class as the objects for studying the specifics of the processes of structure formation during solidification of slowly crystallizing melts. The research of the thermal regime interrelationships with the physical parameters that specify the rate of the melt crystallization is usually carried out by mathematical modeling [5-8].

In this paper, the thermal modes of obtaining and crystallization kinetics of castings are investigated with using a mathematical model of heat transfer and crystallization processes under conditions of melt cast into a metal mold with walls of finite thickness [9]. The calculations were performed in application to a three-component easy amorphizing alloy $Mg_{65}Cu_{25}Y_{10}$. The choice of alloy arises from the fact of presence in literature the temperature dependences of the supercooled viscosity of melted metal and the difference of free energy between liquid and crystalline phases [10], and experimental values of the critical cooling rate and casting section by which an amorphous structure is fixed [11]. The presence of these data suggests, on the one hand, the number reducing of free parameters of the model and thus increasing the level of adequacy, and on the other hand, evaluating the correctness of the calculated analysis results.

2. Characteristics of the model

Physical model assumptions have been formulated on the basis of the one-dimensional scheme of heat extraction from the flat melt layer with $2l_1$ thickness in copper mold with a wall thickness of l_2 (fig. 1). Melt layer was considered to have a certain initial temperature in all volume and to begin cooling simultaneously at all points of contact with the walls of the mold. As the melt conjugation with the heat-conducting walls is not ideal heat transfer conditions in the contact plane were specified by a finite quantity of heat transfer coefficient α_1, which was evaluated by a working procedure [4].

Before melt pouring the mold was assumed to have an initial temperature equal to ambient temperature. At the moment of the thermal contact between the melt and the ingot mold the temperature of border areas increases, whereupon the remote from the contact plane heat receiver zones are heated up. This creates preconditions for heat exchange of the mold with the external environment (still air). The contribution of this effect to the overall picture of the thermal process was determined by the magnitude of the heat transfer coefficient α_2, which values were chosen in accordance with the recommendations of the work [12].

The mathematical model basis was specified by the system of Fourier one-dimensional differential heat conduction equations for the melt containing the source of release of the latent heat of crystallization and copper mold. The basic equations were

supplemented by boundary conditions, which formalize the above mentioned physical assumptions of the model.

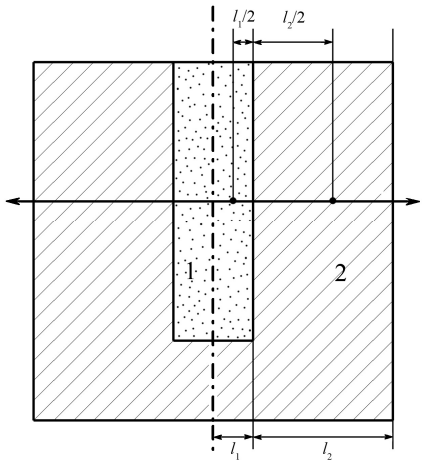

Fig. 1. Scheme section of plane-parallel casting (1) and mold (2): l_1 – half-thickness of casting; l_2 – the thickness of heat-conducting mold wall; ↔ the directions of primary heat-removing; • – points used for the calculation of temperatures T_1 and T_2.

The fraction of volume x, which has been transformed at any given time station t, was calculated in the approximation of the effective nucleation rates and crystal growth [13] with using the integral equation:

$$x(t) = \frac{4}{3}\pi \int_0^t (1 - x(t'))I(t') \left[R_c(t') + \int_{t'}^t (1 - x(t''))u(t'')dt'' \right]^3 dt' \quad (1)$$

where I – the frequency of crystal nuclei formation of critical size R_c; u – crystal growth rate; t_m – time to peak the melting temperature of the molten material T_m; $t' \le t'' \le t$ – current time.

The temperature dependence of the parameters I, R_c , and u included in kinetic equation (1) were specified by the classical crystallization theory [14-16] for homogeneous nucleation mechanisms and normal crystal growth:

$$I_o(T) = \frac{N_v D}{a_o^2} \exp\left(-W / k_B T\right), \quad (2)$$

$$W = \frac{16\pi V_m^2 \sigma^3}{3\Delta G^2}, \quad (3)$$

$$u(T) = \frac{fD}{a_o}\left[1 - \exp\left(-\frac{\Delta G}{RT}\right)\right], \quad (4)$$

$$R_c = \frac{2V_m \sigma}{\Delta G}, \quad (5)$$

where I_o – steady-state nucleation rate; N_v – the number of atoms per unit volume; D – diffusion coefficient at the boundary between the crystal and the melt; a_o – the thickness of the interface, which was identified with the atomic diameter value; W – the work of critical nucleus size formation; V_m – molar volume; σ – the specific surface energy on the boundary of the nucleus-melt; ΔG – molar difference between the free energies of liquid and crystalline phases; f – the fraction of sites on the surface of the crystal where the adjunction of atoms moving from melt (for normal growth mechanism f=1) is possible; k_B – Boltzmann constant; R – universal gas constant.

The effect of the non-stationary distribution of heterophase fluctuations according to the sizes has been taking into account in calculating the nucleation rate in QLS conditions by expression[17]:

$$I = I_o \exp(-\tau / t). \tag{6}$$

The time delay τ, when the stationary distribution of heterophase fluctuations establishes in sizes, were determined from the ratio:

$$\tau = \frac{3\pi^2 V_m \eta(T)}{RT} \tag{7}$$

where η – dynamic viscosity of melt.

As can be seen from the expressions (2) – (5), the basic parameters, i.e. the set of values of the nucleation rate, crystal growth rate, and the critical size of nuclei, are the diffusion coefficient at the interface boundary D, energy transformation stimulus ΔG, and specific free energy of the crystal-melt surface σ. Taking into account the absence of reference information on the diffusion atom mobility at the interface of liquid and crystalline phases, the value D was determined by pre-calculated values of the melt viscosity η with using the Stokes-Einstein relation:

$$D = \frac{k_B T}{3\pi a_o \eta(T)}. \tag{8}$$

In turn, the temperature viscosity dependence was specified by Vogel-Fulcher-Taman equation using η_o, D^*, T_o constants [10], which provide the best agreement between the calculated and experimental data:

$$\eta(T) = \eta_o \exp\left(\frac{D^* T_o}{T_o - T}\right) \tag{9}$$

where η_o=3·10^{-5} Па·с; D^*=22,1; T_o=260 К.

The difference in the Gibbs free energy ΔG was determined from the general thermodynamic principles, based on the ratio:

$$\Delta G(T) = \Delta H_m \frac{T_m - T}{T_m} + \int_{T_m}^{T} \Delta C_p(T')dT' - T\int_{T_m}^{T} \frac{\Delta C_p(T')}{T'}dT'. \tag{10}$$

At that we used the experimentally determined temperature dependence of the specific heat capacity difference between liquid and crystalline phases $\Delta C_p(T)$, values of melting temperature T_m, and the molar fusion heat ΔH_m of $Mg_{65}Cu_{25}Y_{10}$ alloy [10]:

$$\Delta C_p(T) = 0{,}01752 \cdot T + 1{,}8 \cdot 10^6 \cdot T^{-2} - 1{,}02 \cdot 10^{-5} \cdot T^2;$$

here T_m=730 K; ΔH_m=8,65·10^3 J/mol.

The free energy of specific interface σ was considered to be independent from the temperature. The numerical value of this parameter σ=0,068 J/m^2 was found by the method [18].

The thermal and kinetic problems, which are interrelated elements of the above presented model, were solved consistently by the finite difference method using implicit difference scheme [19]. Calculations were performed with using the original program compiled by Object Pascal. More detailed description of the proposed model is presented in [9].

3. The results of calculations and analysis

Modeling results of thermal regimes and crystallization kinetics of $Mg_{65}Cu_{25}Y_{10}$ melt in copper mold were obtained as the graphs of time dependence of casting temperatures $T_1(t)$ and mold temperatures $T_2(t)$, and the fraction of crystallized volume $x(t)$ (Figs. 2, 4, 6). In addition to the basic calculation data, we constructed final values dependencies $x(x_e)$, the number of crystals per volume unit N_S and their average sizes $\bar{R}$ on casting half-thickness l_1 (Figs. 3, 5, 7). Calculations were performed for castings of half-thickness from 0.8 to 8.0 mm, which solidify in the mold with heat-removing walls of thickness l_2 = 15 mm. The temperature values T_1 and T_2 were determined at the points lying at the distances $l_1/2$ and $l_2/2$ from the heat transfer plane (Fig. 1). The initial values of the parameters T_1 and T_2 were specified equal to T_m+100 K=830 K and 293 K, respectively.

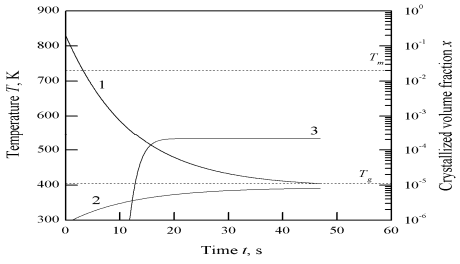

Fig. 2. Calculated dependences on the time of the melt T_1 and the mold T_2 temperatures, and crystallized volume fraction x for castings of $Mg_{65}Cu_{25}Y_{10}$ alloy with half-thickness l_1=4.0 mm: 1 – $T_1(t)$, 2 – $T_2(t)$, 3 – $x(t)$.

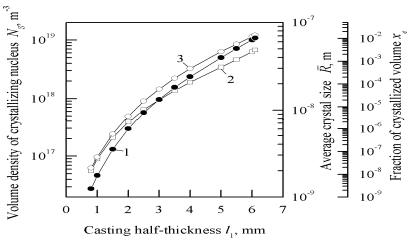

Fig. 3. Calculated dependences of crystallized volume fraction (1), the number of crystals per volume unit (2) and their average sizes (3) on the half-thickness of castings with conventionally amorphous structure.

The analysis of obtained calculated data shows that the castings of 0.8 to 6.1 mm half-thickness solidify in conditions of continuous cooling with a gradually decreasing rate until glass transition temperature T_g of alloy is achieved (Fig.2). In this thermal process regime the typical structure for metallic glasses is fixed. It consists of an amorphous matrix with nano-sized inclusions, so called "quenching nucleus". Their volume fraction does not exceed the level of X-ray diffraction sensitivity (~10^{-2}), so that they are not detected in X-ray diffraction spectra. With the value l_1 increase in the above

mentioned range the volume density of crystallization nucleus increases from ~ $6 \cdot 10^6$ to ~ $7 \cdot 10^{18}$ m^{-3} and their averaged size increases from 2 to 72 nm (Fig. 3). Thus, in spite of impossibility of experimental (XRD) detection of crystal component in $Mg_{65}Cu_{25}Y_{10}$ castings with half-thickness up to 6.1 mm, their structure should be classified as conditionally amorphous one.

The calculated dependence $x_e(l_1)$ was used to determine the critical half-thickness l_1^c of castings, which solidify forming a negligible relative volume of the crystalline phase $x_e \approx 10^{-6}$. Further, according to the value l_1^c, the corresponding critical cooling rate of the melt υ_m^c .was evaluated with using methods [4] The resulting calculation value l_1^c=2 mm and υ_m^c=91.4 K/s were compared with experimental data [11]: $(l_1^c)_{\exp}$=2 mm $(\upsilon_m^c)_{\exp}$=93 K/s. Attained modeling results agreement with experiment prove the correctness of the proposed model and created of its computational algorithm on its basis.

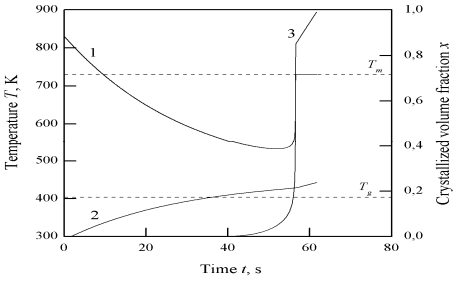

Fig. 4. Calculated temperature results of $Mg_{65}Cu_{25}Y_{10}$ alloy, mold, and volume fraction under crystallization depending on the time for castings solidifying with half-thickness l_1=7,5 mm: 1 – $T_1(t)$, 2 – $T_2(t)$, 3 – $x(t)$.

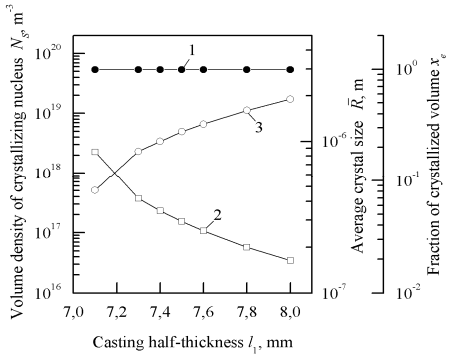

Figs. 5. Calculated dependence of x_e, N_s and $\bar{R}$ parameters on the half-thickness (7,1 ≤ l_1 ≤ 8,0 mm) of completely crystallizing castings: 1 – $x_e(l_1)$, 2 – $N_S(l_1)$, 3 – $\bar{R}$ (l_1).

Figure 4 shows the results of model calculations for castings corresponding to the values l_1 from 7.1 to 8.0 mm. It can be seen that in this case the character of dependences $T_1(t)$ and $x(t)$ changes qualitatively in comparison with similar graphs presented in Fig.2. On the temperature curves after substantial melt supercooling achievement in relation to T_m recalescence areas appear, indicating a sharp temperature increase of crystallizing castings. In turn, the changes in the temperature mode of the process from cooling to heating cause the significant changes in the numerical values of the temperature-dependent parameters of I and u that control the crystallization kinetics.

As the results of a total analysis of the calculated dependences $T_1(t)$, $I(t)$, $u(t)$ show, at the stage of castings self-heating from the point of minimum temperature curve $T_1^{\min}$ to a temperature T_e of the process finish, the formation rate of new crystallization centers is abruptly reduced to almost zero, and the growth rate of crystals, conversely, increases by 1-2 orders of magnitude (Table 1). The important consequences of these changes in the parameters I and u are the termination of the nucleation mechanism, acceleration (due to the increase of the growth rate) and the full completion of the crystallization, as well as reducing the number of crystals per volume unit and increase in their average size (i.e., roughening of the castings microstructure) that is proved by $x_e(l_1)$, $N_S(l_1)$ and $\bar{R}(l_1)$ in Fig.5. As it can be seen from the data presented, the completely crystallizing casting, due

to the above-mentioned features of temperature, attains a microcrystalline structure with average crystal sizes between 0.4 - 0.5 to 2.0 mkm.

Table 1

Changing the frequency of nucleation and crystal growth rate on the recalescence stage process of producing castings of alloy $Mg_{65}Cu_{25}Y_{10}$

l_1, mkm	T_{min}, K	T_e, K	I, $m^{-3}\cdot s^{-1}$		u, $m\cdot s^{-1}$	
			T_{min}	T_e	T_{min}	T_e
7,1	513	729,9	$1{,}45\cdot10^{17}$	0	$1{,}43\cdot10^{-8}$	$5{,}19\cdot10^{-7}$
7,3	526	729,8	$4{,}24\cdot10^{16}$	0	$4{,}36\cdot10^{-8}$	$8{,}34\cdot10^{-7}$
7,5	532	729,7	$2{,}04\cdot10^{16}$	0	$6{,}77\cdot10^{-8}$	$1{,}03\cdot10^{-6}$
8,0	540	729,6	$5{,}41\cdot10^{15}$	0	$1{,}25\cdot10^{-7}$	$1{,}42\cdot10^{-6}$

In the range of values $6{,}2 \le l_1 \le 7{,}07$ mm the character of calculated dependences $T_1(t)$, $T_2(t)$, $x(t)$ indicates the successive development of the two stages of castings solidification. As it can be seen in Fig.6, for a relatively small time intervals $t_f \approx 0{,}04t_e$ where t_e – total process time, the temperatures of crystallizing melt and mold become closer, whereupon their relatively slow ($\sim 9\cdot10^{-3}$ K/s) simultaneous cooling to the glass transition temperature begins. At the initial stage of accelerated $(1–5)\cdot10^{-1}$ K/s cooling parameters I and u are changed, passing through its maximum values. By the time of establishing the mode of coordinated castings and mold cooling, the crystal growth rate is reduced to an extremely low level of $\sim10^{-11}$ m/s, at which crystal growth is largely suppressed while the rate of nucleation retains sufficiently high values $\sim10^{16} – 10^{17}$ $m^{-3}c^{-1}$ (Table 2).

Table 2

Changes the parameters that control the temperature mode and crystallization kinetics, in the first stage solidification of castings half-thickness of 7.0 mm

t/t_f	$T_1(t)$, K	$T_2(t)$, K	$I(t)$, $m^{-3}\cdot s^{-1}$	$u(t)$, $m\cdot s^{-1}$	$x(t)$	x_e
0,05	729	332	0	$4{,}9\cdot10^{-6}$	0	$9{,}9\cdot10^{-2}$
0,07	698	345	0	$4{,}5\cdot10^{-5}$	0	
0,1	653	363	$2{,}0\cdot10^{-32}$	$2{,}2\cdot10^{-5}$	$1{,}1\cdot10^{-50}$	
0,3	516	421	$1{,}2\cdot10^{17}$	$1{,}9\cdot10^{-8}$	$4{,}0\cdot10^{-2}$	
0,41	489	435	$3{,}2\cdot10^{17}$	$1{,}4\cdot10^{-9}$	$8{,}7\cdot10^{-2}$	
0,5	474	442	$2{,}3\cdot10^{17}$	$2{,}4\cdot10^{-10}$	$9{,}3\cdot10^{-2}$	
0,7	458	448	$8{,}0\cdot10^{16}$	$2{,}7\cdot10^{-11}$	$9{,}5\cdot10^{-2}$	
0,9	453	449	$4{,}7\cdot10^{16}$	$1{,}3\cdot10^{-11}$	$9{,}5\cdot10^{-2}$	
1,0	452	450	$4{,}2\cdot10^{16}$	$1{,}1\cdot10^{-11}$	$9{,}6\cdot10^{-2}$	

The final stage of castings solidification is carried out by deep supercooling of the melt with respect to T_m (269–296 K) under conditions of slow temperature drop from $T_1(t_f)$ to T_g. At this part of dependence $T_1(t)$ the increment of crystallized fraction is due to the formation of new crystal nuclei and a very slow enlargement of both newly emerging crystallization centers, and the crystals formed at the initial stage of the process. According to the estimated data, the combined action of the nucleation mechanism and inertly proceeding growth add negligible contribution ~ 0.4% to value x_e.

It follows that in the given castings the majority of transformed volume is formed at the first stage of the process. As a result of its short duration and rapid decrease in the growth rate of ~ $5\cdot10^{-5}$ до ~ 10^{-11} m/s, the sizes of the formed crystals do not exceed ~ 90 nm. At the final stage the further magnitude decline u occurs, thereupon the crystal sizes of this class remain practically unchanged. For the same reason, the sizes of the newly incipient crystals do not substantially change. By the time they reach the glass transition

temperature and the residual liquid phase transition to amorphous state, the maximum values of these crystals R is not more than 20 nm.

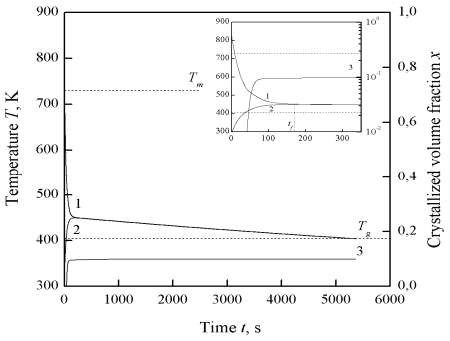

Fig. 6. The results of matching numerical solution of heat and kinetic problems for the manufacturing castings process from $Mg_{65}Cu_{25}Y_{10}$ alloy with half-thickness l_1=7.0 mm. Parameter notations are the same as in Figures 2 and 4. Insert is the initial stage of the process: t_f – time to establish the mode of joint casting and mold cooling.

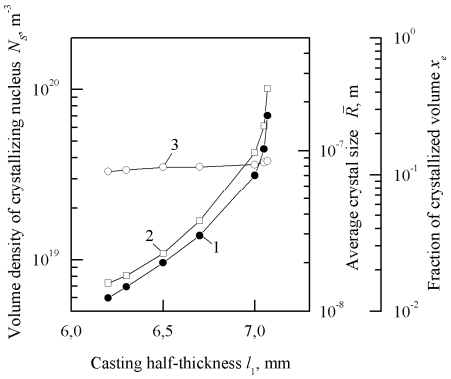

Fig. 7. Changes in fraction of transformed volume x_e, volume density N_s and the average crystal sizes $\overline{R}$ depending on the half-thickness ($6{,}2 \le l_1 \le 7{,}07$ mm) of amorphous-nanocrystalline castings: 1 – $x_e(l_1)$, 2 – $N_S(l_1)$, 3 – $\overline{R}$ (l_1)

As a result of analysis we can conclude that in the castings of $Mg_{65}Cu_{25}Y_{10}$ alloy with half-thickness of 6.2 – 7.07 mm amorphous-nanocrystalline structure is fixed. In this structure the final volume fraction of the crystalline component is greater than the value of ~ 10^{-2}, accepted as an ultimate measure of X-ray analysis sensitivity, but on the other hand, does not exceed the level of 0.99, which in computational algorithms usually serves as the criterion of complete crystallization.

With castings thickness increase in the investigated range of values l_1 the melt supercooling, corresponding to the time of t_f, is reduced from 296 to 269 K, which causes a slight acceleration of the nucleation processes and crystal growth. In addition, the overall duration of the process increases from $t_e = 3.5 \cdot 10^3$ s to $6.4 \cdot 10^3$ s. The cumulative result of changes parameters I, u and t_e is the increase in finite fraction of transformed volume from 0.01 to 0.27, volume density of crystals from ~$7 \cdot 10^{18}$ to ~10^{20} m^{-3}, and their averaged sizes from 74 to 86 nm that is seen from the corresponding graphic dependences, shown in Figure 7.

4. Conclusions

1. The analysis of structure formation processes at casting of light glass transition $Mg_{65}Cu_{25}Y_{10}$ alloy into a metal mold has been done by matching method of numerical solution of heat conduction equation and crystallization kinetics.

2. The formation of three microstructure types: conventionally amorphous ($l_1 \le 6{,}1$ mm; $x_e \sim 10^{-2}$), amorphous-crystalline ($6{,}2 < l_1 \le 7{,}07$ mm; $10^{-2} < x_e \le 0{,}99$), and microcrystalline ($l_1 > 7.1$ mm; $x_e = 0.99$) is possible depending on casting half-thickness ($0.8 < l_1 \le 8.0$ мм).

3. The correspondence of experimental and estimated values of critical thickness and amorphizing cooling rate of castings has been established.

References

1. **Kovneristyy, Yu. K.** Obyemno-amorfiziruyushchiyesya metallicheskiye splavy [Text] / Yu. K. Kovneristyy. – M.: Nauka, – 1999. – 80 p
2. **Inoue, A.** Stabilization of metallic supercooled liquid and bulk amorphous alloys [Text] / A. Inoue // Acta Mater. – 2000. – Vol. 48. – P. 279 – 306.
3. **Miller, M.** Bulk Metallic Glasses [Text] / M. Miller, P. Liaw. – Springer Science Business Media. – 2008. – 237 p.
4. **Lysenko, A.B.** Raschet skorosti okhlazhdeniya pri zakalke splavov iz zhidkogo sostoyaniya [Text] / A. B. Lysenko, G. V. Borisova, O. L. Kravets // Fizika i tekhnika vysokikh davleniy. – 2004. – Vol. 14, No. 1. – P. 44 – 53.
5. **Sellger, R.** Influence of cooling characteristics on glass formation of metallic glasses [Text] / R. Sellger, W. Loser, G. Richter // Mater. Sci. Eng. – 1988. – Vol. 97. – P. 203 – 206.
6. **Tkatch, V. I.** Computer simulation of $Fe_{80}B_{20}$ alloy solidification in the melt spinning process [Text] / V. I. Tkatch, S. N. Denisenko, B. I. Selyakov // Acta Metallurg. Mater. – 1995. – Vol. 43, No 6. – P. 2485 – 2491.
7. **Lysenko, A. B.** Solidification of metals under melt quenching condition [Text] / A. B. Lysenko, G. V. Borisova, O. L. Kravets, A. A. Lysenko// The Physics of Metals and Metallography. – 2008. – Vol.106, No 5. – P. 435 – 443.
8. **Lysenko, A. B.** Vliyaniye termicheskogo rezhima zakalki iz zhidkogo sostoyaniya na mikrostrukturu metallov [Text] / A. B. Lysenko, O. L. Kravets, A. A. Lysenko // Metallofiz. noveyshiye tekhnol. – 2008. – Vol. 30, No 3. – P. 415 – 427.
9. **Lysenko, A. B.** Kinetika kristallizatsii obyemno-amorfiziruyushchegosya splava Cu47Ni8Ti34Zr11 v usloviyakh kokilnogo litia [Text] / A. B. Lysenko, O. L. Kosinskaya, S. V. Gubarev, T. V. Kalinina // Metallofiz. i noveishie tekhnol. – 2014. – Vol. 36, No 10. – P. 1411 – 1425.
10. **Busch R.** Thermodynamics and kinetics of $Mg_{65}Cu_{25}Y_{10}$ bulk metallic glass forming liquid / R.Busch, W.Lin, W.L.Johnson // J. Appl. Phys. –1998. – Vol.83, №8. – P.4134–4141.
11. **Inoue, A.** Mg-Cu-Y amorphous alloys with high mechanical strengths produced by a metallic casting method [Text] / A. Inoue, A. Kato, T. Zhang, S. G. Kim, T. Masumoto // Mater. Trans. JIM. – 1991. –Vol. 32. – P. 609 – 616.
12. **Baskakov, A. P.** Teplotekhnika [Text] / A. P. Baskakov, B. V. Berg, O. K. Vitt. – M.: Energoatomizdat, – 1991. – 224 p.
13. **Lysenko, A. B.** Kineticheskaya model massovoy kristallizatsii v priblizhenii effektivnyy skorostey zarozhdeniya i rosta kristallov [Text] / A. B. Lysenko // Vìsn. Dnìpropetr. Unìv., Ser. Fìz. radìoelektron. – 2011. – Vol. 19, No 2. – P. 3 – 11.
14. **Ovsiyenko, D. E.** Zarozhdeniye i rost kristallov iz rasplava [Text] / D. E. Ovsiyenko. – Kiyev: Naukova dumka, 1994. – 254 p.
15. **Skripov, V. P.** Spontannaya kristallizatsiya pereokhlazhdennykh zhidkostey. [Text] / V. P. Skripov, V. P. Koverda. – M.: Nauka, 1984. – 232 p.
16. **Chernov, A. A.** Protsessy kristallizatsii [Text] / A. A. Chernov // Sovremennaya kristallografiya. Vol.3. – M.: Nauka, 1980. – P. 7 – 232.
17. **Vreswijk, J. C. A**. Nucleation kinetics and critical cooling rate of glass-forming liquids [Text] / J. C.A. Vreswijk, R. G. Gossink, J. M. Stevels // J. Non-Cryst. Solids. – 1974. – No 16. – P. 15 – 26.
18. **Mondal, K.** On the prediction of solid – liquid interfacial energy of glass forming liquids from homogeneous nucleation theory [Text] / K. Mondal, B. S. Murty // Mater. Sci. Eng. A – 2007. – Vol. 454 – 455. – P. 654 – 661
19. **Samarskiy, A. A.** Chislennyye metody [Text] / A. A. Samarskiy, A. V. Gulin. – M.: Nauka, – 1989. – 432 p.

Received 03.05.2016